Materials Engineering

Concepts and Applications

Reece Hughes

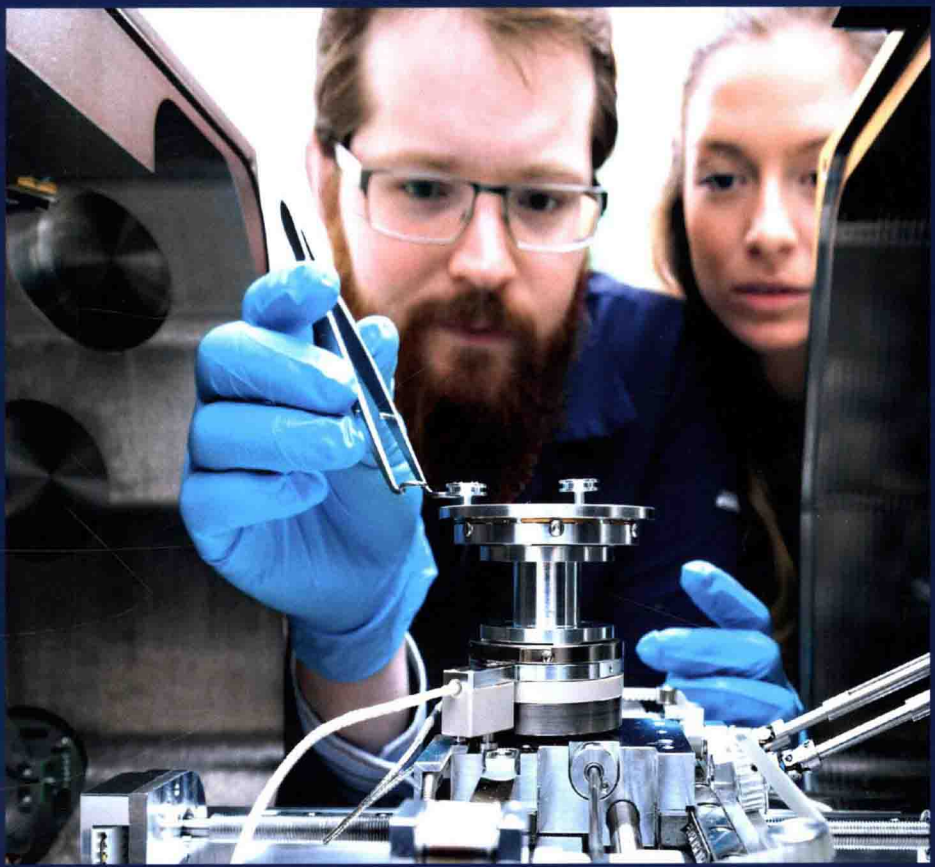

Materials Engineering: Concepts and Applications

About the Book

Materials science is the study of materials, their discovery, design and manufacture with special emphasis being given to solid materials. This book on materials science discusses the advanced principles that determine the structure of particular materials. Allied fields of research in this subject include nanomaterial engineering, biomaterial engineering and optical and magnetic materials engineering. Topics included in this book elucidate the various technologies that are applied at this level. There has been rapid progress in this field and its applications are finding their way across multiple industries. The extensive content of this book provides the readers with a thorough understanding of the subject.

About the Editor

Reece Hughes graduated in the field of materials science and engineering. He serves as a lecturer of materials science in a public research university in Ireland. His expertise and academic interests lie in surface chemistry, surface materials science and nanotechnology. He has attended several international conferences and seminars; and presented over 13 scientific papers at these conferences. Hughes has more than 8 articles, papers and book chapters to his credit.

ISBN 978-1-63238-553-6

NY RESEARCH PRESS
www.nyresearchpress.com

Hughes

Materials Engineering: Concepts and Applications

NY RESEARCH PRESS

Materials Engineering: Concepts and Applications

Editor: Reece Hughes

NY RESEARCH
PRESS
New York

Published by NY Research Press
118-35 Queens Blvd., Suite 400,
Forest Hills, NY 11375, USA
www.nyresearchpress.com

Materials Engineering: Concepts and Applications
Edited by Reece Hughes

International Standard Book Number: 978-1-63238-553-6 (Hardback)

Cataloging-in-Publication Data

Materials engineering : concepts and applications / edited by Reece Hughes.
p. cm.
Includes bibliographical references and index.
ISBN 978-1-63238-553-6
1. Materials. 2. Materials science. 3. Engineering. I. Hughes, Reece.
TA403 .M38 2017
620.11--dc23

Printed in China.

Materials Engineering: Concepts and Applications

Preface

Materials science is the study of materials, their discovery, design and manufacture with special emphasis being given to solid materials. This book on materials science discusses the advanced principles that determine the structure of particular materials. Allied fields of research in this subject include nanomaterial engineering, biomaterial engineering and optical and magnetic materials engineering. Topics included in this book elucidate the various technologies that are applied at this level. There has been rapid progress in this field and its applications are finding their way across multiple industries. The extensive content of this book provides the readers with a thorough understanding of the subject.

This book is a comprehensive compilation of works of different researchers from varied parts of the world. It includes valuable experiences of the researchers with the sole objective of providing the readers (learners) with a proper knowledge of the concerned field. This book will be beneficial in evoking inspiration and enhancing the knowledge of the interested readers.

In the end, I would like to extend my heartiest thanks to the authors who worked with great determination on their chapters. I also appreciate the publisher's support in the course of the book. I would also like to deeply acknowledge my family who stood by me as a source of inspiration during the project.

Editor

Contents

Preface VII

Chapter 1 **Effect of Moisture Exchange on Interface Formation in the Repair System Studied by X-ray Absorption** 1
Mladena Lukovic and Guang Ye

Chapter 2 **Preparation and Characterization of Blended Films from Quaternized Hemicelluloses and Carboxymethyl Cellulose** 18
Xian-Ming Qi, Shi-Yun Liu, Fang-Bing Chu, Shuai Pang, Yan-Ru Liang, Ying Guan, Feng Peng and Run-Cang Sun

Chapter 3 **Inactivated Sendai Virus (HVJ-E) Immobilized Electrospun Nanofiber for Cancer Therapy** 30
Takaharu Okada, Eri Niiyama, Koichiro Uto, Takao Aoyagi and Mitsuhiro Ebara

Chapter 4 **Investigation of High-Energy Ion-Irradiated MA957 using Synchrotron Radiation under *In-Situ* Tension** 41
Kun Mo, Di Yun, Yinbin Miao, Xiang Liu, Michael Pellin, Jonathan Almer, Jun-Sang Park, James F. Stubbins, Shaofei Zhu and Abdellatif M. Yacout

Chapter 5 **Activation of Aspen Wood with Carbon Dioxide and Phosphoric Acid for Removal of Total Organic Carbon from Oil Sands Produced Water: Increasing the Yield with Bio-Oil Recycling** 52
Andrei Veksha, Tazul I. Bhuiyan and Josephine M. Hill

Chapter 6 **Cutting Modeling of Hybrid CFRP/Ti Composite with Induced Damage Analysis** 65
Jinyang Xu and Mohamed El Mansori

Chapter 7 **Preparation and Characterization of Inorganic PCM Microcapsules by Fluidized Bed Method** 87
Svetlana Ushak, M. Judith Cruz, Luisa F. Cabeza and Mario Grágeda

Chapter 8 **A Comparison of Simple Methods to Incorporate Material Temperature Dependency in the Green's Function Method for Estimating Transient Thermal Stresses in Thick-Walled Power Plant Components** 98
James Rouse and Christopher Hyde

Chapter 9 **Facile Synthesis of $SrCO_3$-$Sr(OH)_2$/PPy Nanocomposite with Enhanced Photocatalytic Activity under Visible Light** 117
Alfredo Márquez-Herrera, Victor Manuel Ovando-Medina, Blanca Estela Castillo-Reyes, Martin Zapata-Torres, Miguel Meléndez-Lira and Jaquelina González-Castañeda

Chapter 10 **Improved Electrochemical Detection of Zinc Ions using Electrode Modified with Electrochemically Reduced Graphene Oxide** 130
Jiri Kudr, Lukas Richtera, Lukas Nejdl, Kledi Xhaxhiu, Petr Vitek, Branislav Rutkay-Nedecky, David Hynek, Pavel Kopel, Vojtech Adam and Rene Kizek

Chapter 11 **Heteroatom Doped-Carbon Nanospheres as Anodes in Lithium Ion Batteries** 142
George S. Pappas, Stefania Ferrari, Xiaobin Huang, Rohit Bhagat, David M. Haddleton and Chaoying Wan

Chapter 12 **Preliminary Investigation of the Process Capabilities of Hydroforging** 155
Bandar Alzahrani and Gracious Ngaile

Chapter 13 **Improved Sectional Image Analysis Technique for Evaluating Fiber Orientations in Fiber-Reinforced Cement-Based Materials** 168
Bang Yeon Lee, Su-Tae Kang, Hae-Bum Yun and Yun Yong Kim

Chapter 14 **Correlation of High Magnetoelectric Coupling with Oxygen Vacancy Superstructure in Epitaxial Multiferroic BaTiO3-BiFeO3 Composite Thin Films** 181
Michael Lorenz, Gerald Wagner, Vera Lazenka, Peter Schwinkendorf, Michael Bonholzer, Margriet J. Van Bael, André Vantomme, Kristiaan Temst, Oliver Oeckler and Marius Grundmann

Chapter 15 **Effect of Rare Earth Metals on the Microstructure of Al-Si Based Alloys** 194
Saleh A. Alkahtani, Emad M. Elgallad, Mahmoud M. Tash, Agnes M. Samuel and Fawzy H. Samuel

Chapter 16 **Comparison of Cyclic Hysteresis Behavior between Cross-Ply C/SiC and SiC/SiC Ceramic-Matrix Composites** 207
Longbiao Li

Chapter 17 **Influence of Oxygen Concentration on the Performance of Ultra-Thin RF Magnetron Sputter Deposited Indium Tin Oxide Films as a Top Electrode for Photovoltaic Devices** 220
Jephias Gwamuri, Murugesan Marikkannan, Jeyanthinath Mayandi, Patrick K. Bowen and Joshua M. Pearce

Permissions

List of Contributors

Index

1

Effect of Moisture Exchange on Interface Formation in the Repair System Studied by X-ray Absorption

Mladena Lukovic * and Guang Ye

Academic Editor: Hong Wong

Section of Materials and Environment, Faculty of Civil Engineering and Geosciences, Delft University of Technology, Delft 2628 CD, The Netherlands; g.ye@tudelft.nl
* Correspondence: m.lukovic@tudelft.nl

Abstract: In concrete repair systems, material properties of the repair material and the interface are greatly influenced by the moisture exchange between the repair material and the substrate. If the substrate is dry, it can absorb water from the repair material and reduce its effective water-to-cement ratio (w/c). This further affects the hydration rate of cement based material. In addition to the change in hydration rate, void content at the interface between the two materials is also affected. In this research, the influence of moisture exchange on the void content in the repair system as a function of initial saturation level of the substrate is investigated. Repair systems with varying level of substrate saturation are made. Moisture exchange in these repair systems as a function of time is monitored by the X-ray absorption technique. After a specified curing age (3 d), the internal microstructure of the repair systems was captured by micro-computed X-ray tomography (CT-scanning). From reconstructed images, different phases in the repair system (repair material, substrate, voids) can be distinguished. In order to quantify the void content, voids were thresholded and their percentage was calculated. It was found that significantly more voids form when the substrate is dry prior to application of the repair material. Air, initially filling voids and pores of the dry substrate, is being released due to the moisture exchange. As a result, air voids remain entrapped in the repair material close to the interface. These voids are found to form as a continuation of pre-existing surface voids in the substrate. Knowledge about moisture exchange and its effects provides engineers with the basis for recommendations about substrate preconditioning in practice.

Keywords: moisture exchange; repair system; interface; void content

1. Introduction

Moisture transport between a cementitious repair material and a concrete (or mortar) substrate determines the microstructural development of the interface and repair material in concrete repair systems [1,2]. Still, this area of research remains scarcely understood, because the dynamics of water exchange is very complicated and strongly influenced by hydration of the repair material. Only a few studies on the moisture exchange in multilayer systems when fresh, newly-cast material was placed on the matured substrate have been reported [3–5]. In all of these studies, nuclear magnetic resonance (NMR) technique was used. Some preliminary studies on layered "Lego blocks" specimens made of freshly cast cement pastes were performed by using X-ray absorption [6]. Most of these studies only focused on the moisture exchange: they indicated the relative change of moisture content in the repair system. Effects of the moisture exchange on the microstructure of the interface and repair material were not studied. Interface microstructure between a brick and mortar after moisture movement was only investigated by Brocken *et al.* [3].

The aim of this paper is to study effects of the moisture exchange and the substrate preparation on the interface and repair material formation in a repair system. The X-ray absorption technique is first used to quantitatively study moisture movement in a repair system. Ordinary Portland cement (OPC) paste with w/c of 0.3 is used as a repair material. Samples were sealed for 3 d and during this period the moisture exchange was monitored. Subsequently, the internal microstructure of the repair system is studied by CT scanning in order to investigate the consequences of moisture exchange on the formed structure.

2. Materials and Methods

2.1. *Materials and Sample Prepartion*

The substrate used in the study was a two year old mortar. A standard mortar mixture (OPC CEM I 42.5N (ENCI, Rotterdam, The Netherlands), w/c 1:2, cement-to-sand ratio 1:3) was used. After two years of fog curing (100% relative humidity, temperature 20 °C), two small prism specimens ($18 \times 19 \times 40$ mm^3) were cut with a diamond saw from bigger mortar samples. Prior to casting of the repair material, top surface of the substrate was polished to minimize the influence of surface roughness (Figure 1a). Two samples (marked as S1 and S2) with a sealant on the sides were then placed in a mold and covered with aluminum self-adhesive film (AST) to prevent water evaporation from the sides (Figure 1b). A glass reference was placed between two samples in order to account for variations in the beam intensity, as later explained.

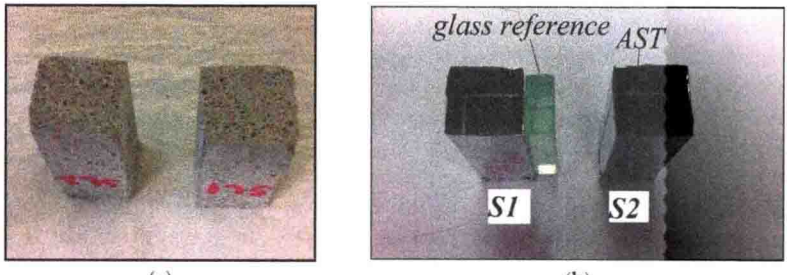

(a) (b)

Figure 1. Preparation of the mortar substrate sample: (**a**) After cutting and polishing; (**b**) In a mold and covered by aluminum self-adhesive tape (AST).

Before covering with AST, mortar substrate was preconditioned in two ways. Dry substrate (DS) simple was dried in an oven at 105 °C until constant weight was achieved. This was done in order to remove all evaporable water and create a zero initial moisture content at the beginning of the experiment [7]. It has to be noted that these conditions might trigger some microstructural changes and microcracking in the material [8]. The other mortar substrate was kept in the fog room prior to casting of the repair material. This substrate was considered as wet (saturated) substrate (WS). For repair materials, cement paste with OPC CEM 42.5 N and w/c of 0.3 was used.

2.2. *X-ray Absorption for Moisture Content Measurements*

After the preparation, two samples and a glass reference were placed in a plastic container (Figure 2a). Subsequently, container is placed in a Phoenix Nanotom X-ray system (Phoenix | x-ray, Wunstorf, Germany, Figure 2b) where water exchange was measured. The apparatus is equipped for Computer Tomography (CT scanning), but in this part of the study was limited to X-ray imaging without specimen rotation. A comparison between two X-ray images taken at the beginning and after a certain time step provides a moisture change in the sample at a certain time step. Even though relative humidity (RH) and temperature (T) are not controlled in the X-ray system, RH

and temperature measuring devices (see in Figure 2b) were placed in an X-ray system chamber during testing.

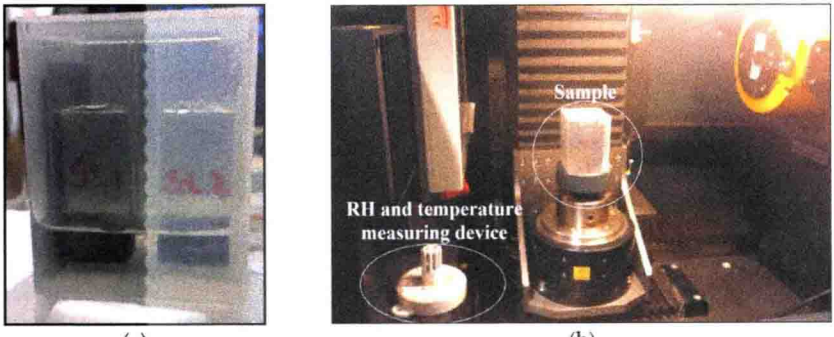

(a) (b)

Figure 2. Samples for moisture exchange measurements; (**a**) two specimens are placed in a plastic container prior to X-ray testing; and (**b**) the X-ray system with the position of the sample and temperature and RH sensors.

When an object is irradiated with an X-ray, the X-ray is attenuated (scattered and absorbed) due to the interaction with the material. The attenuation behavior of monochromatic X-rays (X-ray photons of a single, consistent energy) can be described by the Beer-Lambert law [9]:

$$I = I_0 e^{-\mu d} \tag{1}$$

where μ is the attenuation coefficient; d is the thickness of the sample; and I_0 is the incident intensity. An attenuated X-ray results in transmitted intensity I. Detector visualizes intensities levels as grey scale values (GSV) [10]. Therefore, the attenuation coefficient of material with a known thickness can be determined by knowing the change in intensity level, $ln(I/I_0)$ (Equation (1)), or by knowing the change in GSV, $ln(GSV/GSV_0)$.

During moisture transport (either wetting or drying), GSV of material is changing. Correlating GSV change with the change in moisture content is done by making use of a simple physical principle. In a dry sample, X-rays are attenuated by the dry material only (Figure 3-left). By scanning through the dry material, a reference image is obtained. If water is added to the porous material, the attenuating material will consist of the dry material plus a thickness of a fictitious water layer (d_w), equivalent to the additional moisture content of the material (Figure 3-right) [10]. Additional moisture content is obtained by logarithmically subtracting a reference image from the image taken during moisture exchange. Therefore, provided that the change in beam intensity, $ln(I/I_0)$, and attenuation coefficient of water are known, the (additional) moisture content inside the material can be determined according to Equation (1). In this case I_0 corresponds to beam intensity after passing through the dry material, while I corresponds to beam intensity after passing through the wet material. For quantification of the moisture content change, the following procedure was used.

- The attenuation coefficient of water can be determined based on the GSV change of empty and water filled container with a known thickness (see Figure 4). The following formula can be used:

$$GSV_{water} = GSV_{air} e^{-\mu_{water} d_{water}} \tag{2}$$

where GSV_{water} is the greyscale value of water; GSV_{air} the grey scale value of air; d_{water} is the thickness of water (which is equal to the thickness of the container); and μ_{water} is the attenuation coefficient of water. The first image is made with a beam passing through an empty container

and GSV_{air} (corresponds to I_0) is obtained (Figure 4a). The second image is made with a container filled with water and GSV_{water} (corresponds to I) is obtained (Figure 4b). Thus, the unknown μ_{water} can be calculated based on Equation (2). Note that this equation is equivalent to Equation (1). Further discussion about the attenuation coefficient of water when polychromatic X-ray is used, is given in the following subsection.

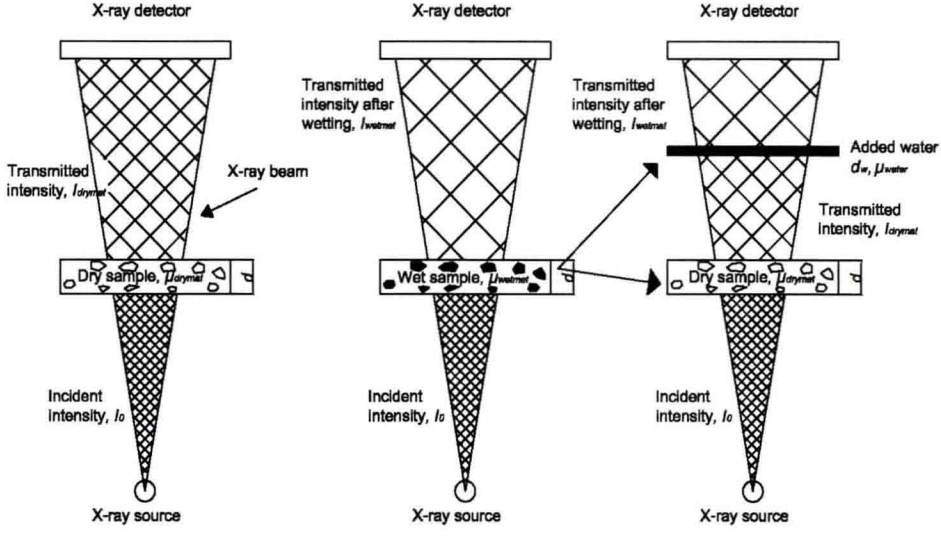

Figure 3. The moisture distribution is obtained by logarithmically subtracting an image of the dry sample I_{dry} from the image of the wet sample I_{wet}, adopted from Reference [10].

- Once the attenuation coefficient of water is determined, GSV of the wet porous material can be correlated to GSV of the dry porous material according to the following equation (also derived from Equation (1)):

$$GSV_{wetmat} = GSV_{drymat} e^{-\mu_{water} d_w} \tag{3}$$

where d_w is the thickness of fictitious water layer equivalent to the additional moisture content in sample (see Figure 3) and can be expressed as:

$$d_w = \Delta c_{water} \frac{d}{\rho_{water}} \tag{4}$$

Here, Δc_{water} is the change of water content (g/cm^3); d is the thickness of the sample; and ρ_w is the density of water. From these equations, Δc_{water} can be determined as:

$$\Delta c_{water} = -\frac{\rho_{water}}{\mu_{water} d} \ln \frac{GSV_{wetmat}}{GSV_{drymat}} \tag{5}$$

- In this study, only the middle part of the specimen (around 16 mm) is analyzed in order to exclude the influence of edges (see Figure 5). Obtained moisture profiles are then averaged over the specimen's width. As a result, the change in moisture content is obtained as function of specimen height.

Due to slight variations in the beam intensity, the obtained GSV varies even without a change in the moisture content. In order to account for this effect, a glass reference was used in all analyses (see Figures 1b and 4a). It is considered that glass does not absorb water and therefore, in this region,

GSV should be constant during the analysis. Therefore, each image was normalized according to the variations of GSV of the glass reference in order to account for changes in the beam intensity.

The parameters for X-ray analysis were set as: X-ray tube voltage 130 kV, X-ray tube current 270 μA. The spatial resolution was 30 μm/pixel. Each image used in the analysis (a representative image) is an average of 25 images. With 0.5 s needed for acquisition of an image, a representative image for a certain time step was obtained in 12.5 s.

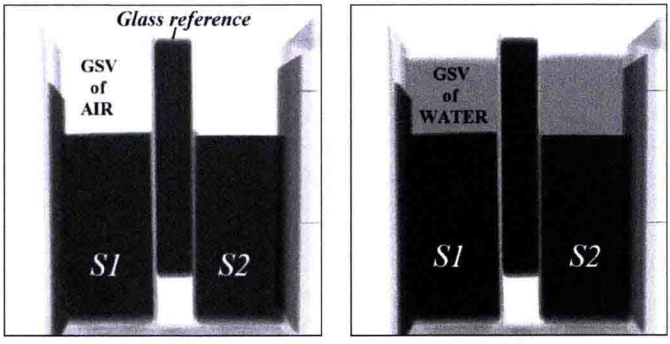

(a) (b)

Figure 4. Difference in GSV between an empty and water filled container placed at the top of the samples S1 and S2, used for calculating attenuation coefficient of water: (**a**) GSV of an empty container; and (**b**) GSV of water-filled container.

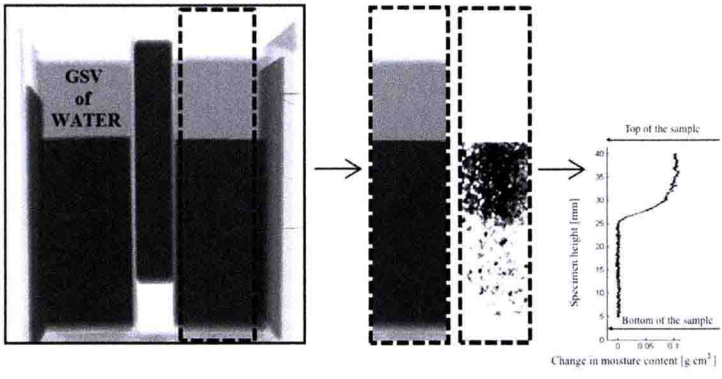

Figure 5. An example of the original X-ray image and analyzed part of the specimen from which the moisture profile is calculated.

2.2.1. Determination of the Attenuation Coefficient

When using polychromatic X-ray source (photons emitted over a spectrum of energy levels), such as the one used in this research, two aspects should be considered in order to determine the attenuation coefficient of water [11].

The first aspect is that the attenuation coefficient of water depends on the water layer thickness. This dependency is a consequence of using polychromatic X-ray source which leads to so called "beam hardening" effect: while photons are passing through the material, lower energy X-ray photons are attenuated easier, the energy spectrum is changing, and progressively, with increasing thickness of material, remaining protons become "harder" to attenuate. As a result, the measured attenuation coefficient will depend on the thickness of the material. Attenuation provided by a certain

thickness of a material is described by the term "effective attenuation coefficient". Pease *et al.* [11] observed that, with the increasing thickness of the water (and also other materials such as clay brick, concrete, and wood), the effective attenuation coefficient of material decreases. The effective attenuation coefficient of water in this research, measured for the different water layer thickness (Figure 6), shows the same behavior.

The second aspect is related to the beam-hardening effect and the widely used non interacting composite system (Figure 3), which assumes that the porous parent material does not influence the attenuation coefficient provided by water. In the absorption (or drying) tests, however, photons are attenuated both by the parent material and the water. Therefore, the attenuation coefficient of water cannot be determined independently of the parent material (in this case mortar substrate). In order to account for this, Pease *et al.* [11] introduced the term called "coupled effective attenuation coefficient" of water which is a function of the parent material and its thickness. They observed that, with increasing thickness of different materials (e.g., concrete, cement paste, calcium silicate, *etc*), the coupled effective attenuation coefficient of water decreases. In this research, the same was tested by placing the 18 mm thick mortar substrate in front of the water holder (with inner dimensions of 4 mm, 9 mm, and 33 mm). The obtained coupled effective attenuation coefficient of water was lower than the effective one (Figure 6), similar to findings of Pease *et al.* [11].

As the thickness of the water layer should be similar to the anticipated maximum change of the water content in the parent material, the attenuation coefficient of the 4 mm thick water layer, placed behind the 18 mm thick mortar substrate (0.1728 cm^{-1}) was used further to quantify the change of the water content. Accordingly, the maximum change of the water content in the mortar substrate is assumed to be around 0.22 g/cm^3, which should be reasonably close to the maximum moisture content of the mortar.

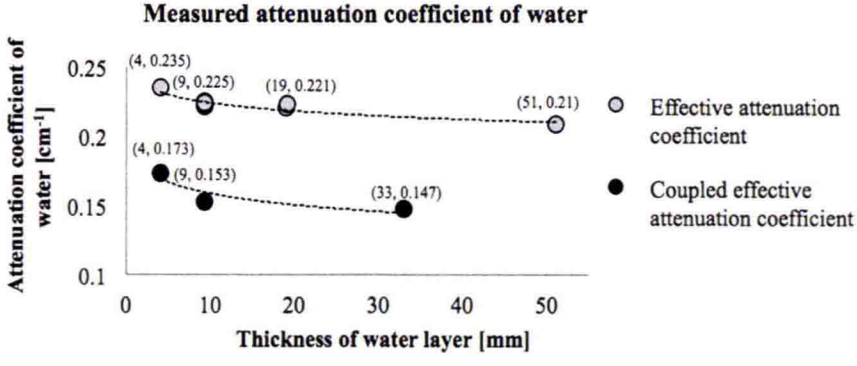

Figure 6. Influence of water layer thickness and parent material (mortar substrate) on measured attenuation coefficient of water.

2.2.2. Limitations of the Experiment

An important limitation of this technique is caused by the conical beam of the X-ray setup. As a result, the thickness of the material through which the beam passes depends on the position of the source with respect to the specific location (*i.e.*, coordinate) in the sample (Figure 7a). Consequently, at the top and the bottom of the sample, the thickness of the attenuating material is larger, and this will affect the effective attenuation coefficient. The thickness of the sample through which the beam is passing varies between 18 mm in the middle of the specimen (*i.e.*, when the beam is perpendicular to the specimen) and 18.16 mm at the top and bottom (Figure 7). In the current research, this was not taken into account, but should be considered for improvement of the technique.

One more consequence of the conical beam is that X-ray photons are not emitted parallel to the repair/substrate interface. The interface location, therefore, is not well defined, and it includes a